Full Title: THE RELATION BETWEEN LAND-COVER AND THE URBAN HEAT ISLAND IN NORTHEASTERN PUERTO RICO

Short Title: LAND-COVER AND THE URBAN HEAT ISLAND IN NORTHEASTERN PUERTO RICO

David J. R. Murphy[1*], Myrna Hall[1], Charles Hall[1], Gordon Heisler[2], Steve Stehman[1], and Carlos Anselmi-Molina[3]

[1*]301 Illick Hall, SUNY- College of Environmental Science and Forestry, Syracuse, NY, 13210, Phone: (315) 412–4619, Fax: (315) 470-6934, Email: djmurp03@syr.edu
[2]U.S. Forest Service, 5 Moon Library, SUNY-ESF, Syracuse, NY, 13210
[3] Physics Building, Marine Science Department, University of Puerto Rico Mayaguez, Puerto Rico, 00681-9000

Sponsors: This research was supported financially by the United States National Science Foundation (NSF) Luquillo (LUQ) Long Term Ecological Research Program in Puerto Rico, Grant Number BSR-8811902, DEB 9411973, DEB 0080538, and DEB 0218039. Equipment for this research was provided by Dr. Jorge Gonzalez of Santa Clara University, and Dr. Gordon Heisler of the United States Forest Service.

Abstract. Population movements, growth and industrialization are causing rapid urbanization throughout the tropics, resulting in elevated temperatures within urban areas when compared to surrounding rural areas, a phenomenon known as the Urban Heat Island (UHI). One such example is the city of San Juan, Puerto Rico. Our objective in this study is to quantify the UHI created by the San Juan Metropolitan Area over space and time using temperature data collected by mobile and fixed-station measurements. We used the fixed-station measurements to examine the relation between average temperature at a given location and the density of vegetation located upwind. We then regressed temperatures against regional land-cover to predict future temperature with projected land-cover change. Our data show the existence of a nocturnal UHI, with nighttime urban-rural temperature differences ($\Delta T_{U\text{-}R}$) of up to 3.02°C. Urban-rural temperature differences had negligible seasonal differences. Comparisons of diurnal temperature trends at urban, grassland, and forested sites indicate that canopy cover reduced daytime warming. Results from the mobile measurements show that the UHI has reached the base of the Luquillo Mountains. Temperature was predicted best ($r^2 = 0.94$) by vegetation in upwind easterly directions, especially that within 180 meters of the sensor. Predictions of future development and temperatures suggest that if the present pattern of development continues, over 140 km^2 of land that showed no signs of UHI in 2000 will have an average annual UHI between +0.4°C and +1.55°C by 2050. Furthermore, more than 130 km^2 of land area with a current UHI between +0.4°C and +1.4°C in 2000 will have an average UHI greater than +1.55°C by 2050.

Keywords: Urban Heat Islands, land-cover, sky view factor, GEOMOD, urban climate, temperature measurements, urbanization

1. INTRODUCTION

As development continues in Puerto Rico, forests and grasslands are being converted to non-vegetated cover, changing the magnitude and geographic range of the excess urban temperature phenomenon known as the Urban Heat Island (UHI). This study aims to quantify the spatial and temporal variations of the UHI in and around the San Juan Metropolitan Area (SJMA). From this we wish to assess the present, and potential future, range of the UHI and the impacts it may impart on the nearby tropical forest ecosystem, which is the site of the U.S. National Science Foundation supported Luquillo -Long Term Ecological Research Program. Our specific objectives are to: (1) quantify the magnitude and timing of the peak diurnal and seasonal urban heat island created by the SJMA, (2) explore correlations between air temperature and land-cover, (3) assess the geographic range of the UHI created by the SJMA, and (4) predict the growth of the geographic range of the UHI into the future.

An important reason for studying the UHI in Northeastern Puerto Rico is that much of the freshwater for the SJMA originates in the Luquillo Mountains, located 17 kilometers to the east of the SJMA (Figure 1). This water supply is barely adequate in dry years. There is new concern that overall precipitation trends within Puerto Rico during the 20th century have decreased about 16% (van der Molen, 2002) and that three of the top ten driest years in the past century were recorded in the 1990's (Larsen, 2000). Furthermore, a growing body of evidence suggests that urbanization may affect regional climates even more than increasing global temperatures (Hulme and Viner, 1995; Scatena, 1998; Brazel *et al.,* 2000). Therefore, we believe that research efforts should focus not only on global climate change, but also on the regional climatic effects of urbanization, especially the effects of UHI's.

Anthropogenic alterations to the earth surface cause microclimatic changes that result in the formation of Urban Heat Islands (Landsberg, 1981). Land-cover types common to urban areas, such as dark colored pavement, brick, and asphalt, absorb large amounts of incident radiation during the day and release it as long wave radiation (heat) during the evening, causing maximum temperature differences between urban and rural environments to occur at night (Chandler, 1965; Oke and East, 1971; Landsberg, 1981; Roth, 2007). Reduced longwave cooling caused by diminished sky view factors and materials with high thermal inertia in urban areas also contribute to the UHI effect.

Urban areas tend to remain warmer throughout the evening, making the diurnal (intra-day) range of air temperatures smaller in urban areas when compared to surrounding rural areas in the same locale. Chandler (1965) studied the London UHI over a 10-year period and found that on most days the difference in daily minimum temperature between an urban and rural location was larger than the difference in daily maximum temperature. In a different study, Oke and East (1971) compared the diurnal cooling rates (°C/hour) for three meteorological stations placed in rural, suburban, and urban sites and found that both the rural and suburban locations had decreasing temperatures by 1700 hours while the urban area temperature did not decrease, but in fact increased until 2200 hours.

Anthropogenic heat release can also cause inter-day fluctuations in UHI intensity. Mitchell (1961) showed that differences in daily minimum temperature between the city of New Haven, Connecticut, and a neighboring airport (a non-urban site) were consistent for all days except Sunday, for which it was half as great. Landsberg and Brush (1980) found similar results for Baltimore, Maryland. Both studies concluded that the UHI intensity is more severe on weekdays due to an increase in anthropogenic activity, such as use of automobiles and office air conditioners, which release large amounts of heat into the atmosphere.

Synoptic effects that modify wind speed and atmospheric stability, in addition to the intra- and inter-day trends discussed earlier, impact UHI formation. Oke (1976) found that as wind speed increases, the temperature differential between urban and rural sites ($\Delta T_{U\text{-}R}$) decreases asymptotically. More recently, Comrie (2000) measured the effect of winds on the urban heat island in Tucson, Arizona, and found that even in the presence of strong katabatic flows from surrounding mountains (12m/s), the central city can still maintain urban temperatures 2°C warmer than upwind rural areas. Another recent study by Morris *et al.* (2001) in Melbourne, Australia, found that the UHI was proportional to the inverse of the third root of the wind speed.

The atmospheric factors that influence the intensity of the UHI are summed up by indices of atmospheric thermal stability such as the Turner Class (TC), which is a general measure of stability based on regional wind speed, cloud cover, and time of day. Turner Classes range from 1-7, with 1 being unstable atmospheric conditions, 4 neutral atmospheric conditions, and 7 stable atmospheric conditions (Panofsky and Dutton 1984). Heisler *et al.* (2006) found that the average temperature difference between urban and rural locations in Baltimore, Maryland, was 3.7°C with a stable Turner Class (TC = 7) and only 1.4°C with a neutral Turner Class (TC = 4).

The intensity of UHI's depends on the land-cover characteristics of both rural reference sites and urban sites, and most recent studies used either fixed stations or mobile measurements, or a combination of both, to study the relation between land-cover and the UHI. For example, Hawkins *et al.* (2004) used fixed stations to study the specific effects of different land-cover types in rural landscapes on temperature. When compared to temperature at an urban reference, they found significant differences (~3.4°C) in the UHI ($\Delta T_{U\text{-}R}$) depending on cover type, with the smallest to the largest occurring between the urban reference and hardpan dirt, cultivated vegetation and a mowed grass field, respectively.

Hedquist and Brazel (2006) used a combination of fixed stations and mobile measurements to study the change in temperature, also in Phoenix, Arizona, between urban, residential neighborhoods and rural landscapes. Their data showed an average urban-rural ($\Delta T_{U\text{-}R}$) temperature difference of ~7°C and an urban-residential neighborhood ($\Delta T_{U\text{-}RES}$) temperature difference of ~3°C. In our research we extend the methods used in these studies to examine the UHI in the tropical city of San Juan, Puerto Rico.

The UHI in San Juan, Puerto Rico, was recently studied by González *et al.* (2005) and Velazquez-Lozada *et al.* (2006). Gonzalez *et al.* (2005) used a combination of in situ surface air-temperature data and Airborne Thermal and Land Applications Sensor (ATLAS) data during February, 2004, to study the San Juan UHI. Their results show a late morning peak in the UHI. This finding contradicts much of the aforementioned literature on UHIs that report the peak UHI during the evening hours (Chandler 1965; Oke and East 1971; Landsberg 1981). González *et al.* speculate that the late morning peak was due to low thermal storage caused by a lack of tall skyscrapers, as well as the ability of the UHI to dominate the sea breeze effect, which under normal conditions, would refresh the urban area with cool sea breezes during the day. However, the daytime UHI temperature differences presented by González *et al.*, which included data from four sensors, were just 2.5 ºC or less, and much of this difference may be caused by radiation effects on the sensors if they were differently shaded.

Velazquez-Lozada *et al.* (2006) used a combination of 4 co-op stations and a Regional Atmospheric Modeling System (RAMS) to assess the magnitude of the UHI created by San Juan and its impacts on regional climate. They found that San Juan has been warming at rate of 0.06°C yr^{-1} over the last 40 years, and predicted that the UHI in the SJMA may be as much as 8°C warmer than surrounding rural areas by 2050. We continue the work of González *et al.* (2005) and Velazquez-Lozada *et al.* (2006) by assessing quantitatively the UHI created by the city of San Juan, using both fixed-stations and mobile measurements.

2. STUDY AREA

Puerto Rico is the smallest of the Greater Antilles Island chain, and is located between the Caribbean Sea and the Atlantic Ocean, at 18° north latitude and 66° west longitude. San Juan, the capital and largest city, is located on the eastern half of the island along the north coast. Trade winds from the southeast at low elevations (<300 meters) and from the northeast at high elevations (>300 meters) along with strong afternoon shore breezes dominate mesoscale wind regimes (Odum, 1970; Brown, 1983). There are two mountain ranges on the Island. The 'Luquillo Mountains', which contain the Luquillo Experimental Forest (LEF), are located 17 kilometers east of the San Juan Metropolitan Area (SJMA) and have a maximum elevation of ~1100 meters. The Mid-Island Mountains begin about 60 kilometers southwest of San Juan, and extend through the center of the island, with a maximum elevation of ~1300 meters.

Average temperatures for Puerto Rico range from 24 – 29˚C year round, with a moderate dry season from February till April. Roth (2007) used the Köppen climate classification system to correlate the UHI and urban climates around the world, and according to the average temperature and precipitation regimes in Puerto Rico, most areas are, on average, either 'Am' – tropical monsoon or the 'Af' – wet tropical. The difference between these two classifications depends on the precipitation totals during the dry times of the year, where Af requires greater than 6 cm of precipitation in the driest month (Akin, 1990). According to this system, the San Juan Metropolitan Area the areas out to the east of the San Juan Metropolitan Area in which we did our study, are both classified as Af, 'Wet Tropical' (Table 1).

3. METHODS

We employed two methods to capture the variation of the UHI over space and time: (a) a series of fixed-station temperature sensors (HOBO's), and (b) a series of mobile measurements from a vehicle-mounted temperature sensor (Figure 1a and 1b, Table 1).

3.1 Fixed-Station Measurements

The overall goal of the fixed-station transects was to establish simultaneous temperature measurements to assess the timing of the peak diurnal and seasonal UHI and the influence of land-cover on temperature. The fixed station measurements consisted of a network of ten automated Series-8 HOBO Pro-Temp Data Loggers (Onset Corporation, Pocasset, MA), calibrated to each other and to the ASOS sensor at San Juan airport, to record temperature measurements near different types of land-cover ranging from the center of San Juan to barely developed regions 20 km to the east of the city center. We attached the HOBO sensors to telephone poles about 3 meters above the ground surface. The sensors were all placed within 50 meters of sea level, so elevation should not influence our results. Air temperature measurements were logged automatically at 5 minute intervals, and then aggregated into hourly averages for data analysis. We did not measure humidity because temperature was the primary focus of this study and because the atmospheric controls on humidity are varied and different than that for temperature.

The intensity of UHI's is related to sky view (Landsberg, 1981). Where sky view is restricted by buildings, out-going thermal radiation is restricted at night, turbulent exchange is reduced, and thermal radiation is emitted from vertical building surfaces. To estimate sky view at the sites, we mounted a fish-eye lens on a digital camera to take photographs from which we calculated sky view factor for CBD, HOBO 6S (mowed-grassland) and the Forest site (Figure 2), and using those photographs as a reference, we made visual estimations of the sky view factor for all other sites (Table 1). To estimate sky view, we used the Gap Light Analyzer program (www.ecostudies.org/gla/).

Due to the large geographic extent of San Juan, we decided to establish a series of sensors within a small urban center to the east of San Juan and compare that temperature data to the sensor at the central business district of San Juan (Figure 1a and 1b). The sensors were placed downwind (to the west) of various land-cover types, including urban, grassland, and forest cover (Table 1). These correspond generally to those found in the 2000 land cover classification done by Helmer and Ruefenacht (2005) that would form the basis of our spatial land cover/temperature/up-wind fetch assessment model. We placed the

HOBOs to the west of the various land-cover types selected, with the assumption that the trade-winds would dominate and that the shore breeze, coming mainly from the north, would not be a factor. This wind pattern was supported by observations during the study period and by data collected *post hoc* showing the wind coming from easterly directions over 80% of the time during our sampling period (Figure 3). The wind measurements used in this calculation were taken from the airport, which is located closer to the shoreline then any of our stations. Therefore, we believe that if the airport is not recording shore-breezes, neither will our sensors be impacted by this phenomenon.

The forest, our control, is a lowland old growth forest located between a residential community and an industrial park. It is a remnant of the original natural environment of pre-development Puerto Rico. We recorded measurements here and at ten developed sites during the summer months from June 26th till July 5th and July 10th till July 20th. From September 10th till October 7th we recorded temperature measurements at 6 different locations to add greater spatial coverage to the data set. Comparisons between data collected at the 10 summer and 6 fall locations are believed to reflect spatial differences only since the average temperature in Puerto Rico for the months of July, August and September is 83.0, 83.2, and 83.0, respectively (NCDC, 2007). We also used 5 HOBOs to record data during the months of March and April to gauge dry season effects on the UHI. By using the same stations for both the dry and wet season, we assume that any inter-seasonal temperature differences are due to seasonal effects only and not spatial effects.

The HOBO temperature loggers had internal sensors that, according to the manufacturer's specifications, have a 90% response time in still air of up to 35 minutes and an accuracy of ± 0.2 °C over the range of temperatures measured in Puerto Rico. The error would be larger if radiation errors were present, but we placed the loggers in naturally ventilated radiation shields provided by Onset specifically to reduce radiation-caused error. Temperature measurements collected during calibration exercises performed in a laboratory resulted in an average standard deviation among all sensors of 0.11°C.

3.2 Mobile Measurements

The goal of the mobile data collection was to capture the current geographic range of the UHI. For the mobile measurements we attached an external thermistor temperature probe to a PVC pipe about one meter above the roof of a Jeep Cherokee. A cable from the thermistor probe ran down the PVC pipe into the passenger side window, where it was connected to a data logger that recorded measurements automatically every minute. Since there was good ventilation of the sensor as the vehicle was moving, the response time was not a critical factor.

We collected data by driving along different routes radiating out from the central business district (CBD) of the SJMA to three different surrounding rural areas using an average speed of less than 56 kilometers per hour (35 miles per hour), which was chosen based on similar studies conducted by Oke (1976). In order to drive out to the rural areas and return to the starting point within a reasonable time, we chose mid-size roads, with two lanes in each direction. For each mobile measurement we averaged the values from the departure and return trip so as to avoid any temperature drift due to the change in time between start and end points, which was generally less than one hour each way (elapsed time of < 2 hours). In order to minimize synoptic impacts on UHI formation, the mobile measurements were performed only during evenings with a Turner class of either 6 or 7, indicating relatively stable atmospheric conditions. We replicated each mobile measurement twice, so with three transects and three time periods we made a total of 18 trips. The times of each trip were 0400 – 0600 (pre-sunrise), 1200 – 1400, and 1800 – 2000 (post-sunset). The temperature data were averaged between both replicates and regressed against distance from city center to test whether there is a pattern of cooling as distance from city center increases.

4. UP-WIND FETCH MODEL

We measured the 10 meter wind direction at the San Juan International Airport to be on average from the east during our period of study (Figure 3), and because of the importance of upwind land cover on the magnitude of UHIs found in other studies (Summers, 1964; Oke, 1976; Comrie, 2000; Morris, 2001; González *et al.* 2005, Heisler *et al*., 2006, 2007), we explored correlations between the percent vegetation upwind from each sensor and the average temperature measured at each sensor. To do this we developed a computer model in FORTRAN-90 language that calculated the percent of vegetation within a wedge-shaped upwind area, termed "upwind fetch wedge". The percent vegetation is derived from a year 2000 raster land-cover map of Puerto Rico (Helmer and Ruefenacht, 2005), and is calculated according to:

$$\text{Percent vegetation upwind} = \frac{\text{Number of vegetated pixels within upwind fetch wedge}}{\text{Total number of pixels within upwind fetch wedge}} * 100$$

The model analyzed the percent vegetation over a total of 180 azimuth degrees, from due north to due south, and from zero to a maximum of 2520 meters upwind from each sensor. To do this we divided the 180 azimuth degrees into 18 windows of 10 degrees each, termed "degree windows", and divided the "upwind distances" into 84 intervals of 30 meters each (Figure 4). Due to the predominance of easterly trade winds during our study period (>80% of the time during the study the winds were coming from the east), we limited the model to upwind fetch wedges in easterly directions. At each pixel representing a HOBO sensor on the land-cover map, the model calculated the percent vegetation within all possible upwind fetch wedges. This amounts to 1512 calculations at each sensor (18 degree windows * 84 upwind distances).

We assumed that vegetation in the upwind direction would create lower temperatures whereas impervious surfaces would create higher temperatures at the downwind HOBO sensor. To measure this we regressed the average temperature from the sample period as the dependent variable against percent vegetation as the independent variable and calculated the coefficient of determination, r^2. The regression model is,

$$T = \alpha + \beta x$$

where: "T" is the average temperature (collected by HOBOs 1S to 6S and 1A to 4A during the summer), "x" is the percent vegetation, "α" is the y intercept, and "β" is the slope parameter characterizing the relationship between average temperature and percent vegetation. Thus, the sample size was 10 values of average temperature and percent vegetation for each of 1512 regressions, one regression for each distance and direction from the HOBO sites.

The output of this analysis was 1512 r^2 values from which the highest was picked and assumed to represent the area of upwind fetch to have the most influence on the sensible temperature downwind. This was termed the “best-fit” upwind fetch wedge. All 1512 r^2 values were grouped into 9 classes for ease of graphical visualization and plotted in a gradient space dimensioned by azimuthal degree on the y-axis and upwind distance on the x-axis (see Figure 10, explained in section 5.3). A limited validation of the regression analysis is available from the six fall HOBO stations, which were not used to develop the regression models. For each of these six stations, we calculated the percent vegetation for the “best-fit” upwind fetch wedge and inserted those values into the regression equations to predict temperature. These predicted temperature values were compared to the actual observed average temperature value collected at each of the fall stations

4.1 Predicting the Future UHI

We used the GEOMOD module within the IDRISI Kilimanjaro mapping software (based on Hall *et al.,* 1995; Pontius *et al.* 2001) to predict urbanization (i.e. the number of developed pixels) to the year 2050 in Northeastern Puerto Rico. GEOMOD uses a suitability map as the decision criteria to predict land-cover change over time. Our suitability map represents the ability of any pixel on the land-cover map to change from its current land-cover to an urban land-cover (Pontius *et al.*, 2001). The relative level of suitability for each pixel on the map was based on five variables: slope, aspect, distance to roads, distance to urban areas, and distance to coast, which were derived from the 2000 land-cover map, a map of the current road coverage, and a digital elevation model. Each predicted map of urbanization is based on the suitability map from the previous time step.

For example, the urbanization predicted in 2010 will be used to generate the suitability map used to predict urbanization for the year 2020. We predicted urban growth at decadal intervals starting with the 2000 land-cover map and ending in year 2050. We derived a 'business as usual' rate of urbanization for this model by subtracting urban areas in a 1991 land-cover map from urban areas in the 2000 land-cover map and adjusting the results to decadal intervals.

Using each future land cover map we used the regression results to predict average summer temperature at each pixel as a function of the percent vegetation in the "best-fit" upwind fetch wedge. In order to show the geographic growth of the UHI explicitly over time, we subtracted the average forest temperature (from our measurements at HOBO 2A) from all pixels on the temperature maps to represent the average temperature departure from the lowland forest ecosystem. This statistic is reported as an UHI index.

5. RESULTS AND DISCUSSION

The major findings of this study are: 1) San Juan, Puerto Rico, exhibits an urban heat island of 1.7°C on average during the night, and about 0.93°C on average during the day. 2) The UHI stretches to at least the base of the Luquillo Mountains during the early evening. 3) "Green spaces" were ineffective in combating warming during the day, while only the presence of trees and shading were successful agents in defeating daytime warming. 4) Land-cover up to 180 meters upwind predicted downwind temperature the best ($r^2 = 0.94$). 5) Predictions of future development and temperatures suggest that if the present pattern of development continues in Puerto Rico, over 140 km^2 of land that showed no signs of UHI in 2000 will have an average UHI between +0.4°C and +1.55°C by 2050.

Furthermore, more than 130 km^2 of land area with a UHI between +0.4°C and +1.4°C in 2000 will have an average UHI greater than +1.55°C by 2050.

5.1 Fixed Measurements

Our results show the existence of a pronounced nocturnal UHI (Table 2). The UHI, calculated as the difference in temperature from the central business district (CBD) of San Juan to all other HOBOs ($\Delta T_{CBD\text{-}HB}$), was 1.70°C on average during the early night (1900 to 2359) and 1.81°C during the late night to early morning hours (0000 to 559). Daytime (0600 to 1859) UHI effects were only 0.93°C. Thus the night UHI is twice as great as the day UHI, which is consistent with UHI theory and previous literature (Chandler 1965; Oke and East 1971; Landsberg 1981). Individual values of $\Delta T_{CBD\text{-}HB}$ were highly variable ranging from 0.31°C at the HOBO 4S (residential) to 3.02°C at HOBO 6F (rural commercial). The larger $\Delta T_{CBD\text{-}HB}$ values at night were calculated between the CBD and stations in open, vegetated areas, rather than the forested or thickly vegetated areas, which echo previous findings by Hawkins *et al.* (2004). Large sky view factors at the stations in the open, vegetated areas allow also for enhanced longwave cooling and thus decrease the temperatures quickly after sunset.

$\Delta T_{CBD\text{-}HB}$ was greatest during the wet season (Figure 5). Differences between wet and dry season $\Delta T_{CBD\text{-}HB}$ were less than 1°C on average, and overall were greatest during the early night, followed by the late night, and finally the daytime. We expected the dry season to show higher $\Delta T_{CBD\text{-}HB}$ such as been found in other cities (Roth, 2007). This is a phenomenon due to generally higher thermal inertia and higher humidity levels in wet periods, both of which should decrease rates of cooling in rural areas. However, upon further investigation, the dry season in Puerto Rico is moderate, and we think that our results indicate that wet to dry season differences in a given year can be small, and in fact, it is entirely possible that the rainfall totals at our sites were similar during both the wet and dry seasons. For example, Figure 6 shows the precipitation totals for three different lowland (elevation < 100 meters) stations within the San Juan Metropolitan Area during March of our data collection period. Two of these stations, San Juan Intl Airport and WFO San Juan, are located within 3 km of each other, and the third station, Rio Piedras, is located less than 10 km from either of the other stations.

Although precipitation was recorded often throughout the month, it occurred at all three stations on only 3 of 31 days in March (Days 14, 28 and 30). Large differences in precipitation occur between even the two closest stations, San Juan Intl Airport and WFO San Juan. Precipitation was recorded at either the San Juan Intl Airport or WFO San Juan stations on 18 days in March, however on only half of those days was precipitation recorded at both stations, indicating that a distance of less than 3 km can lead to somewhat substantial differences in precipitation. Furthermore, the largest rain events of the month occurred on two of the three days in which rainfall occurred at all three stations (Days 28 and 30). These results indicate that large synoptic rainfall systems precipitate more uniformly across the region, while smaller, daily rainfall patterns are more random.

Therefore we conclude that: 1) using precipitation gauges near our stations (even within 3km) to represent the average precipitation at our temperature sensors will most likely lead to largely incorrect estimates, as the spatial pattern of daily rainfall for non-mountainous Puerto Rico is non-uniform and almost random. 2) Due to the small size and varying intensity of the rain cells in Puerto Rico, it is also entirely possible that the rainfall total in one area will not be close to the rainfall total in another area only a kilometer away. For these reasons we did not try to correlate regional precipitation totals with our temperature measurements.

We compared the central business district (CBD), HOBO 2A (old-growth forest), HOBO 1S (abandoned agricultural fields), and HOBO 6S (mowed-grassland) diurnal temperature data by hour to view the effects of different land-cover types on air temperature over the day (Figure 7). As expected, the CBD was warmer than all other sites throughout the day and night, emphasizing the impacts of the thermal storage capacity of the large urban area. The grassland site had high daytime air temperatures and low nighttime temperatures, while at the forest site temperatures were consistently cooler and at the CBD consistently warmer throughout both the day and night. These trends resulted in large diurnal temperature ranges at grassland sites, and small diurnal temperature ranges at both the forest and CBD sites (Figure 8). The diurnal temperature trends described here are mainly the result of the balance between insolation and thermal storage capacity. The urban site receives large amounts of insolation on average and is able to retain that energy in the urban materials present, such as cement, asphalt, etc. However the grassland sites that receive equal amounts of insolation do not show large UHI values at night due to very low thermal storage capacity. Furthermore, a lower sky view factor at the urban site (68.8%) compared to the mowed-grassland site (82.5%) will slow longwave cooling at night, increasing the UHI. The forest achieves low temperatures during the day and night by retaining moisture and limiting overall insolation (sky view factor = 6.8%).

According to these results, the presence of grass-covered ‘green space’ will not impede daytime warming. This can be a problem for businesses and homeowners that operate air conditioning units during daytime hours, and whose properties are normally not surrounded by canopy cover. Our results concur with those of Akbari *et al.* (2001) who showed that shading and evaporative cooling, both provided in large amounts by trees, are essential to negate the effects of urban warming. This suggests that "greening" efforts to combat UHIs in the tropics need to focus on increasing tree-cover instead of simply creating park-like 'green spaces'.

5.2 Mobile Measurements

An analysis of the data from the mobile transects ($\Delta T_{CBD\text{-}Tr}$) shows considerable variation in temperature (Figures 9a – 9c), but a clear pattern of cooling with distance from urban center. Thus the UHI decreases as distance from urban center increases. This trend is strongest between 0400 and 0600 hours (~2.5°C) and weakest between 1200 and 1400 hours (<1°C), which agrees with the fixed-station results showing a nighttime peak in UHI intensity, with less difference mid day.

We found negligible cooling along the East Route (Rio Grande in Figure 1) between the hours of 2000 and 2200 (Figure 9c), demonstrating that the UHI effect is strong along this highly developed route during the early evening. Throughout the Rio Grande area especially, there are very large areas of new dense suburban housing and commercial developments, which are most likely adding to the evening warming trend. The Rio Grande route ends at the base of the Luquillo Mountains (Figure 1a); thus an evening UHI extends to the foothills of the Luquillo Mountains. If this pattern of development continues, the temperature increases that accompany the UHI may begin to have impacts on climate patterns in the mountains, such as orographic cloud formation and precipitation. At this time, however, we are unable to assert whether the UHI is impacting precipitation within the Luquillo Mountains.

5.3 Modeling Future Temperature

The best-fit regression ($r^2 = 0.94$) between up-wind vegetation and average temperature at the sensors was obtained using degree window 11 (angle = 101° - 110°, essentially east by southeast, at a distance of 180 meters upwind; Figure 10). Predicted temperature at the 6 fall data sites, calculated using the "best-fit" regression, differed from actual average temperature collected at the 6 stations by an average of only 0.36°C, with a standard error of 0.2.

Assuming no change in vegetation type in the unchanged pixels, our maps projecting future UHI in northeastern Puerto Rico (see Section 3.1) show intensification of the UHI within the SJMA and geographic expansion of the UHI, especially towards the Luquillo Mountains (11a – f). The greatest changes predicted between years 2000 and 2050 are marked by large decreases of land area with a UHI index equal to or less than +0.2°C, and large increases of land areas with a UHI index of +1.55°C. Over 140 km^2 with an UHI index of +0.2°C are converted to land-cover with a higher UHI index, while an additional 130 km^2 is converted to a land-cover with a UHI index of +1.55°C.

The largest changes in the projected UHI index between 2000 and 2050 occur in the +0.2 °C category. This means that urbanization is expanding geographically into presently vegetated areas rather than becoming more intense within previously established urban or suburban areas. Much of this projected urbanization is concentrated in lands to the southeast of the CBD, towards the Luquillo Mountains, which is consistent with our observations. Our results relating land-cover and the UHI, in addition to those of Scatena (1998) who found that land-cover change throughout the island is influencing cloud formation and rainfall patterns within the Luquillo Mountains, highlight the need for research that explicitly studies the effect of land-cover change on precipitation within the Luquillo Mountains.

6. CONCLUSION

Both fixed-station and mobile temperature measurements showed the presence of a nocturnal peak in UHI intensity. The fixed-station data showed also that the UHI peaks during the wet season, which is understandable given the moderate nature of the Puerto Rican dry season. Regional drying due to global climate change, however, may reduce dry season precipitation, and, in line with common findings of other studies, increase the seasonal UHI. The forested site was the coolest on average and able to negate all effects of daytime warming within the canopy layer. This effect occurs because of the absorption of incident solar radiation in the upper tree canopy, where much of it is converted to latent heat via evaporative cooling, thus preventing penetration of solar radiation to warm the soil surface and thus be converted to sensible heat to the air near the ground. Grassland sites showed significant daytime warming, but also pronounced nighttime cooling, resulting in large diurnal temperature ranges. Canopy cover should therefore be encouraged in order to maintain cooler temperatures throughout the day, thus reducing expenditures on air conditioning.

The report by the 2007 Intergovernmental Panel on Climate Change (IPCC, 2007) predicted that global temperatures will increase by 0.2°C per decade. At this rate the global temperature will increase by 1°C by 2050. However, the UHI in Northeastern Puerto Rico is already increasing daily temperatures by more than 2°C in many locations. Furthermore the UHI is expected to expand geographically by 2050, raising daily temperatures between 0.2°C and 1.5°C over much of Northeastern Puerto Rico. According to the findings in this study, development projects encroaching on the Luquillo Mountains may impact regional climate more in the next half century then the changes brought by global climate change. Future research efforts should focus on the specific effects of deforestation, suburbanization, and urbanization on the urban boundary-layer heat island and its effect on lifting condensation levels so as to provide more detailed information pertaining to the future of the freshwater supply for the SJMA.

7. ACKNOWLEDGMENTS

This study was supported in part by the U.S. National Science Foundation through the Long Term Ecological Research Project in the Luquillo Mountains of Puerto Rico, under grants BSR-8811902, DEB 9411973, DEB 0080538, and DEB 0218039. We also thank all of the people who provided help in the field, including Dr. Ricardo Morales, Pieter Van der Meir, Manual Sanfiorenzo, and Dr. Jorge González for lending us the equipment to make this study possible.

8. REFERENCES

Akbari H, Pomerantz M, Taha H. 2001. Cool surfaces and shade trees to reduce energy use and improve air quality in urban areas. *Solar Energy* **70:** 295 - 310.

Akin, Wallace E. 1990. *Global Patterns: Climate, Vegetation, and Soils*. University of Oklahoma Press, Norman. pp 370.

Brazel AJ, Selover N, Vose R, Heisler G. 2000. The tale of two climates - Baltimore and Phoenix urban LTER sites. *Climate Research* **15:** 123-135.

Brown S, Lugo AE, Silander S, Leigel J. 1983. Research history and opportunities in the Luquillo Experimental Forest. Southern Forest Experimental Station, New Orleans, Louisiana. United States Forest Service

Chandler TJ. 1965. *The Climate of London*. Hutchinson.

Comrie AC. 2000. Mapping a wind-modified urban heat island in Tucson, Arizona (with comments on integrating research and undergraduate learning). *Bulletin of the American Meteorological Society* **81:** 2417-2431.

González J, Luvall JC, Rickman D, Corazamy D, Picón A, Harmsen E, Parsiani H, Vasquez RE, Ramírez N, Williams R, Waide RW, Tepley CA. 2005. Urban heat islands developing in coastal tropical cities. *EOS, Transactions, American Geophysical Union* **86:** 397-403

Hall CAS, Tian H, Qi Y, Pontius G, Cornell J. 1995. Modeling Spatial and Temporal Patterns of Tropical Land Use Change. *Journal of Biogeography* **22:** 753-757.

Hawkins TW, Brazel AJ, Stefanov WL, Bigler W, Saffell EM. 2004. The role of rural variability in urban heat island determination for Phoenix, Arizona. *Journal of Applied Meteorology* **43:** 476-486.

Hedquist BC, Brazel AJ. 2006. Urban, residential, and rural climate comparisons from mobile transects and fixed stations: Phoenix, Arizona. *Journal of the Arizona-Nevada Academy of Science* **38:** 77-87.

Heisler G, Walton J, Grimmond S, Pouyat R, Belt K, Nowak D, Yesilonis I, Hom J. 2006. Land-cover influences on air temperature in and near Baltimore, MD. *6th International Conference on Urban Climate,* Gothenburg, Sweden, 392-395. [also available http://www.gvc2.gu.se/icuc6//index.htm].

Heisler G, Walton J, Yesilonis I, Nowak D, Pouyat R, Grant R, Grimmond S, Hyde K, Bacon G. 2007. Empirical modeling and mapping of below-canopy air temperatures in Baltimore, MD and vicinity. *Seventh Urban Environment Symposium*, San Diego, CA, American Meteorological Society, Boston. [http://ams.confex.com/ams/pdfpapers/126981.pdf]

Helmer EH, Ruefenacht B. 2005. Cloud-free satellite image mosaics with regression trees and histogram matching. *Photogrammetric Engineering and Remote Sensing* **71:** 1079–1089.

Hulme M, Viner D. 1995. A climate change scenario for assessing the impact of climate change on tropical rain forests. A report for the World Wildlife Service by the Climatic Research Unit, School of Environmental Sciences, University of East Anglia, Norwich, UK.

Intergovernmental Panel on Climate Change (IPCC). 2007. Climate Change 2007: The Physical Science Basis. http://www.ipcc.ch.

Landsberg HE. 1981. *The Urban Climate*. Vol. 28, *International Geophysics Series* Academic Press.

Landsberg HE, Brush DA. 1980. Some observations of the Baltimore, Md., heat island. *Inst. Phys. Sci. Technol. Tech. Note*, University of Maryland.

Larsen MC. 2000. Analysis of 20th century rainfall and stream flow to characterize drought and water resources in Puerto Rico. *Physical Geography* **21:** 494-521.

Mitchell JM. 1961. The temperature of cities. *Weatherwise* **14:** 224-229.

Morris CJ, Simmonds GI, Plummer N. 2001. Quantification of the influences of wind and cloud on the nocturnal urban heat island of a large city. *Journal of Applied Meteorology* **40:** 169-182.

National Climatic Data Center (NCDC). 2008. National Oceanic and Atmospheric Administration (NOAA). http://www.ncdc.noaa.gov/oa/ncdc.html

Odum HT, Drewry G, Kline JR. 1970. Climate at El Verde, 1963 - 1966. *A Tropical Rain Forest: a study of irradiation and ecology at El Verde, Puerto Rico*, H. T. Odum, Ed., Division of Technical Information, U.S. Atomic Energy Commission.

Oke TR. 1976. The distinction between canopy and boundary layer urban heat islands. *Atmosphere* **14:** 268-277.

Oke TR, East C. 1971. The urban boundary layer in Montreal. *Boundary Layer Meteorology* **1:** 411-437.

Panofsky HA, Dutton JA. 1984. *Atmospheric Turbulence*. John Wiley, 397 pp.

Pontius Jr., RG, Cornell JD, Hall CAS. 2001. Modeling the spatial pattern of land-use change with GEOMOD2: application and validation for Costa Rica. *Agriculture, Ecosystems, and Environment* **85:** 191-203.

Roth, Matthias. 2007. Review of urban climate research in (sub)tropical regions. International Journal of Climatology **27**: 1859-1873

Scatena FN. 1998. Climate change and the Luquillo Experimental Forest of Puerto Rico: assessing the impacts of various climate change scenarios. *American Water Resources Association TPS* **98:** 193-198

Summers PW. 1964. An urban ventilation model applied to Montreal. Ph.D. Dissertation, McGill University.

van der Molen MK. 2002. *Meteorological Impacts of Land Use Change in the Maritime Tropics*. Academisch Proefschrift, Vrije Universiteit, Amsterdam, The Netherlands, 262 pp. [Available at http://www.geo.vu.nl/~moli/PhD/index_PhD.html.]

Velazquez-Lozada A, González J, Winter A, 2006: Urban heat island effect analysis for San Juan, Puerto Rico. *Atmospheric Environment* **40:** 1731-1741.

Table 1. List of all HOBOs and the predominant local land cover. "S" designates HOBO locations during the "summer" data collection period, and "F" designates HOBO locations during the "fall" data collection period. "A" designates the 'additional' HOBOs used during both the summer and fall data collection periods. The site titles, listed under "Land-Cover" were assigned according to the dominant land-cover to the east, as that was found to be the most influential on downwind temperature.

HOBO ID	Land-Cover	Detailed Site Description
1S	Abandoned agricultural fields	Thickly vegetated fields with multiple types of long grass species. Few trees present. Sky view factor greater than 75%. No buildings. One single-lane asphalt road.
2S	Urban Center	Intersection of two single-lane old asphalt roads. Buildings on three of four corners, with a building road ratio of about 1:1, with one larger church steeple, at a building road ratio of 2:1. Sky view factor greater than 50%.
3S	Industrial	<500 meters downwind of a major pharmaceutical plant. A single one-story building near sensor. Mainly grass and bushy vegetation surrounding nearby building. Sky view factor greater than 75%. Building-road ratio around 1:1
4S	Residential	Hobo was placed on a one-lane road bisecting two neighborhoods, one directly east and one directly west. Building-road ratio of about 1:1, and a sky view factor >50%.
5S	Major road crossing	Intersection of two four-lane roads. Car traffic extremely high during rush hours. Two-story mall located 300 meters southeast, and an industrial complex located 400 meters northeast. Sky view factor greater than 50%. Buildings too far for a building road ratio.
6S	Mowed-grassland	Mowed grassland located approx. 200 meters south of a major shopping center, and about 50 meters south of the parking lot for the shopping center. Vegetated hills to the east and south, about 30 meters in height, and covered approximately 30% by trees. Sky view factor of 82.5% (Figure 2).
1A	San Juan Central Business District (CBD)	Located at the intersection of one large road and one side street. Small trees line the south side of the side street, and also the west side of the large road, but do not limit sky view much. Two large buildings to the southeast and southwest have building road ratios of about 8:1, while the building to the northeast has a ratio of 3:1. Sky view factor of about 68.8% (Figure 2).
2A	Old-growth forest	HOBO placed on tree trunk 10 - 20 meters below a full canopy and about 30 meters from the edge of the forest. Broadleaf, climax tree species dominate. Sky view factor is 6.5% (Figure 2).
3A	Grassland mix	This site is located 15 meters south of the old growth forest. There is a field of short grass species to the east, and an industrial complex directly to the west. Sky view factor greater than 50%, with a building road ratio of 1:1.
4A	Residential Limits	HOBO placed at the northern end of a residential neighborhood. The area due east and northeast is wild grassland with sparse tree coverage for +5 Km upwind. Housing structures about 100 meters south. Placed near one short tree (about 4 meters high). Sky view factor greater than 75%
1F	Residential Recreation Park	HOBO placed in neighborhood recreational park. There is a baseball field and basketball court to the south and one-story houses to the north. The sky view factor is greater than 75%.
2F	Residential Church	HOBO placed on a two-lane road adjacent to a house and church. Little vegetation at this site, including only a few trees and shrubs. Building:road ratio is 2:1 Sky view factor greater than 75%.
3F	Suburban Mix	HOBO is located in the eastern side of a small commercial area. One story houses are located to the north, 2 story commercial buildings are located to the east, a small one story shopping center is located to the west, and a cemetery is located to the south. Overall the site has less than 20% vegetation ground cover. Building:road ratio is 1:1. Sky view factor is greater than 75%.
4F	Rural Road	HOBO is located adjacent to a one-lane road, with large trees located to the north, trees and one-story houses located to the south, and a truck stop located to the west. Sky view factor is greater than 50%
5F	Major Road	HOBO is located 1 meter north of a four-lane highway with a few trees. The sky view factor is greater than 75%.
6F	Rural Commercial	HOBO was placed on a short, dirt cross road connecting a one-lane road to a gas station. Mainly grass and bushes surround the HOBO. A four-lane highway is located 100 meters to the north, a one-lane road is located 30 meters to the west, and a gas station is located 50 meters to the east. Sky view factor is greater than 75%.

Table 2. Average temperature difference calculated as urban reference – (individual HOBOs) for all HOBOs along the urban to rural gradient. Maximum and minimum values for each time period indicated in parentheses.

HOBO	Local Land Cover	UHI (°C), ΔT_{CBD-HB}		
		Wet Season		
		Early Night UHI (1900 - 2359)	Late Night UHI (0000 - 559)	Day UHI (0600 - 1859)
1S	Abandoned agricultural fields	1.25	1.47	0.97
2S	Urban Center	0.71 (min)	0.83 (min)	0.55 (min)
3S	Industrial	1.32	1.61	0.90
4S	Residential	0.31	0.64	0.25
5S	Major road crossing	0.78	0.93	0.55
6S	Mowed-grassland	2.44	2.43	0.91
2A	Old-growth forest	2.14	1.86	2.23 (max)
3A	Grassland mix	1.47	1.44	1.10
4A	Residential Limits	2.01	1.76	1.81
1F	Residential Recreation Park	2.05	2.28	0.80
2F	Residential Church	1.47	1.74	0.55
3F	Suburban Mix	1.69	1.90	0.51
4F	Rural Road	2.09	2.42	0.65
5F	Major Road	3.01 (max)	2.80	1.02
6F	Rural Commercial	2.79	3.02 (max)	1.20
	Average ± Standard Error	*1.70 ± 0.19*	*1.81 ± 0.17*	*0.93 ± 0.13*
		Dry Season		
2A	Old-growth forest	1.78	2.02	1.77 (max)
3F	Suburban Mix	0.86 (min)	1.32 (min)	0.40
4F	Rural Road	1.21	1.95	0.34 (min)
5F	Major Road	1.95 (max)	2.27 (max)	0.77
6F	Rural Commercial	1.48	2.22	1.00
	Average ± Standard Error	*1.46 ± 0.19*	*1.96 ± 0.15*	*0.86 ± 0.26*

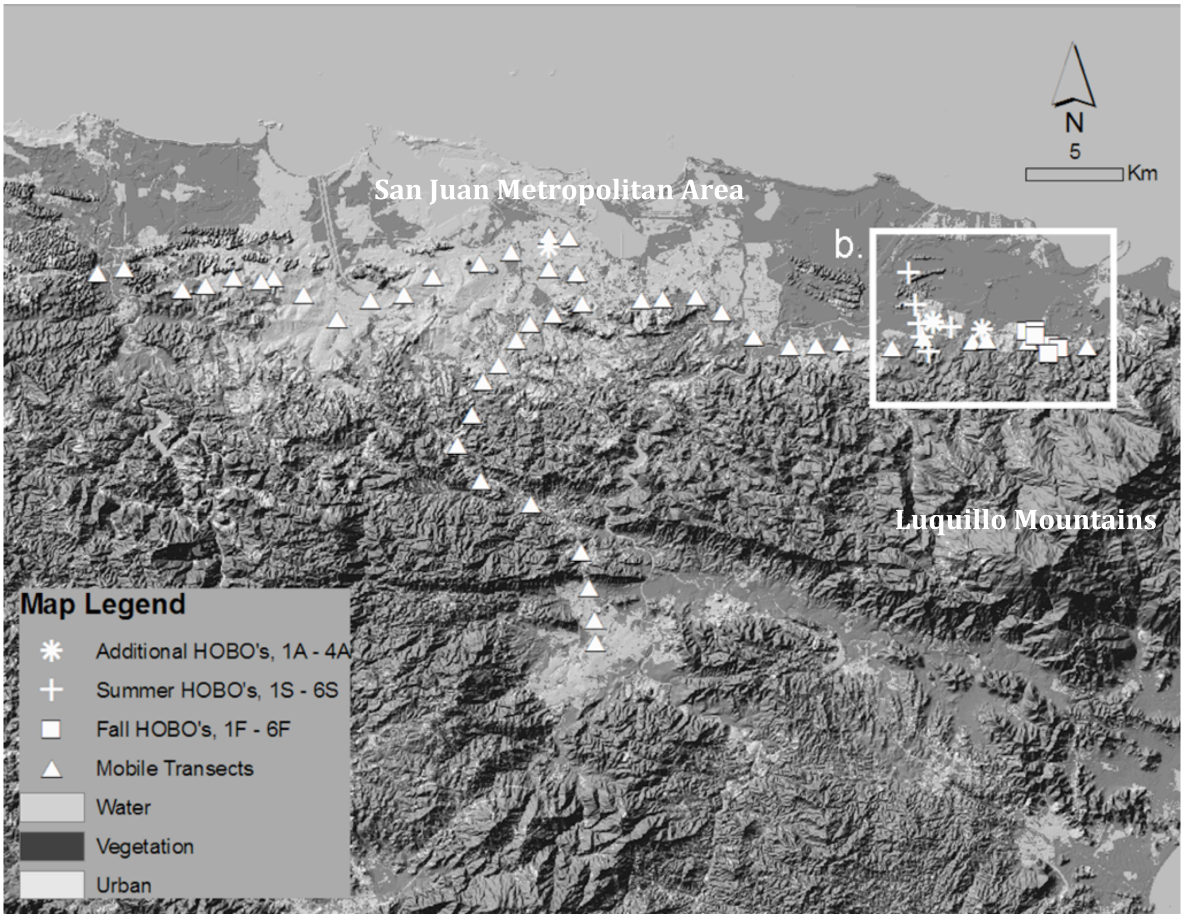

Figure 1a. Land-cover map of Northeastern Puerto Rico with triangles labeling checkpoints along the mobile transects. The crosses, asterisks, and squares mark the locations of the HOBOs. The box represents the area magnified in figure 1b.

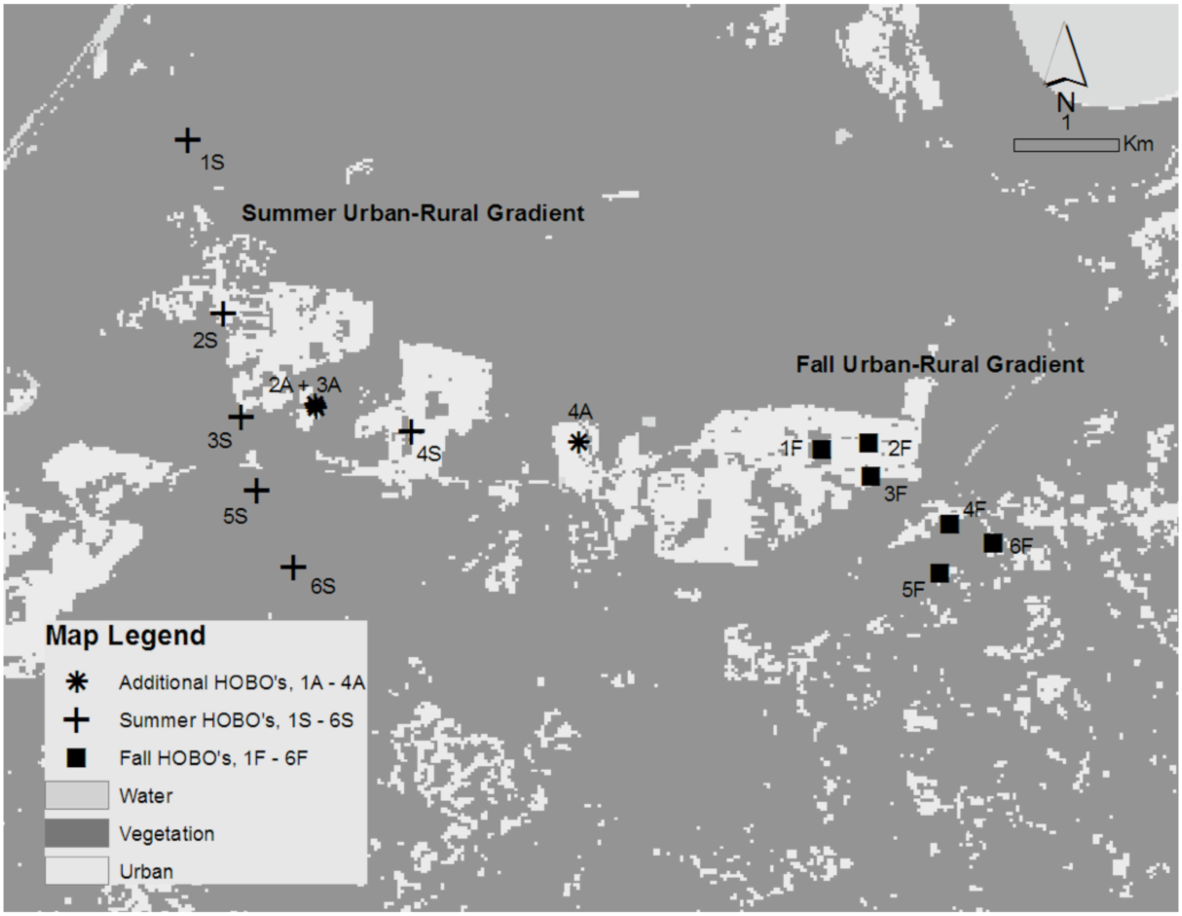

Figure 1b. This is a map of fixed-station measurements. The crosses, labeled HOBO 1S – 6S, were moved during the fall and became HOBO 1F – 6F. The "additional HOBOs", 1A – 4A (1A shown in Figure 1), remained at the same locations for both the summer and fall data periods.

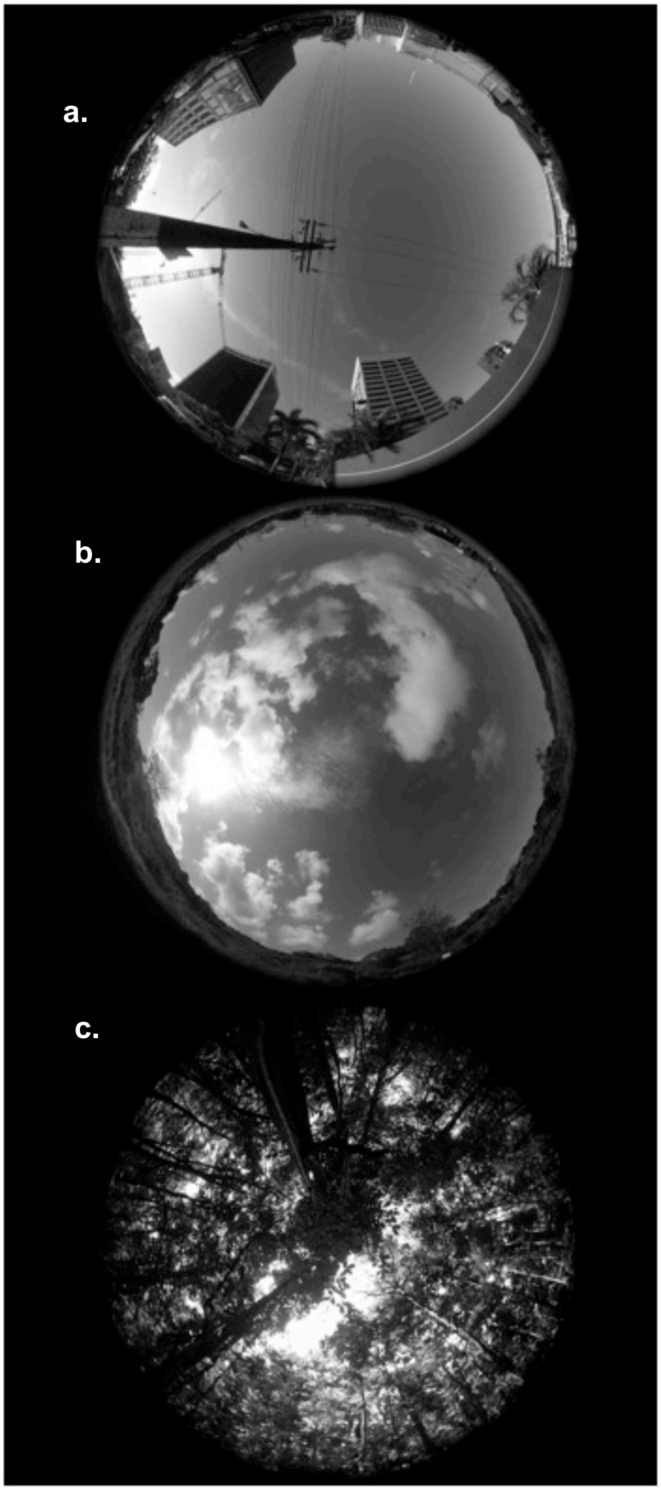

Figure 2. Fish-eye photos of the a) CBD site, b) HOBO 6S (mowed-grassland), and c) the forest site. Sky view factors for each respective site are a) 68.8% b) 82.5% and c) 6.5%

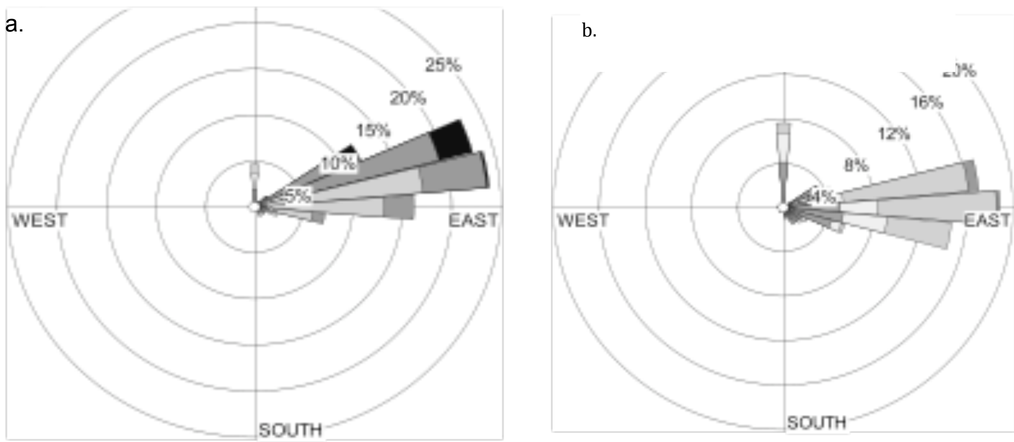

Figure 3. Sample of wind speed and direction distribution at 10 m above ground at the San Juan Marin Airport during July 2006 during day (a) and at night (b). Dotted circles indicate the percentage of time that winds remained at a particular direction, with 10-degree resolution of the wind direction report. Daytime windspeeds peaked at up to 21 knots, whereas nighttime wind speeds did not exceed 17 knots. When wind speed was measureable, but wind direction was too variable to report a given direction, we assigned a direction of 0, which accounts for the winds direction from the north in the graphs.

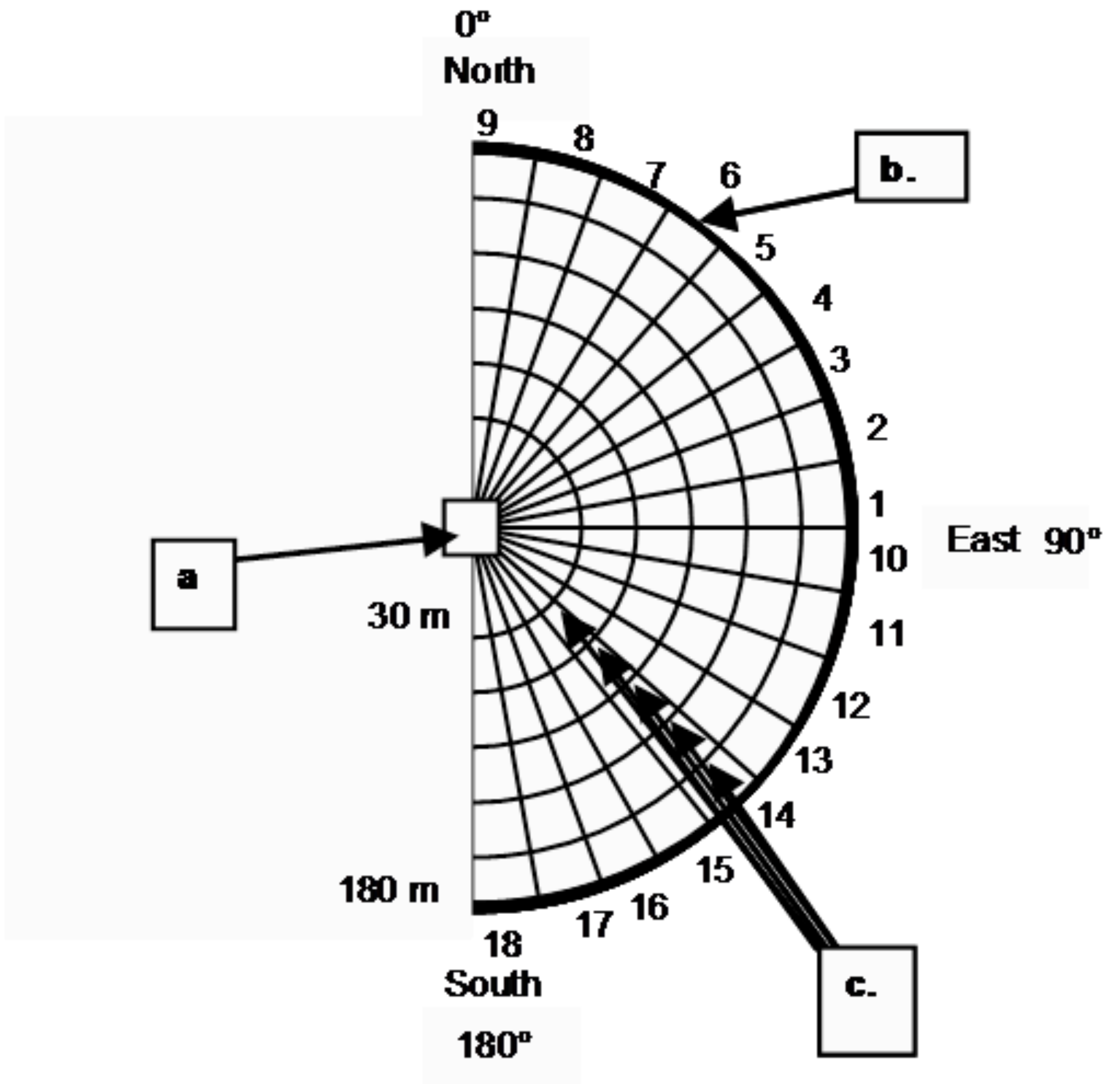

Figure 4. Conceptual diagram of the upwind fetch wedge model. (a) Center pixel, i.e. location of HOBO for regression analysis , (b) Degree Window: 180 degrees azimuth divided into 18 degree windows of 10° each, numbered here as 1 – 18. (C) Upwind Distance: 30 meter increments away from center pixel to a maximum of 2520 meters upwind, totaling 84 different distances upwind (only first 6 distances shown).

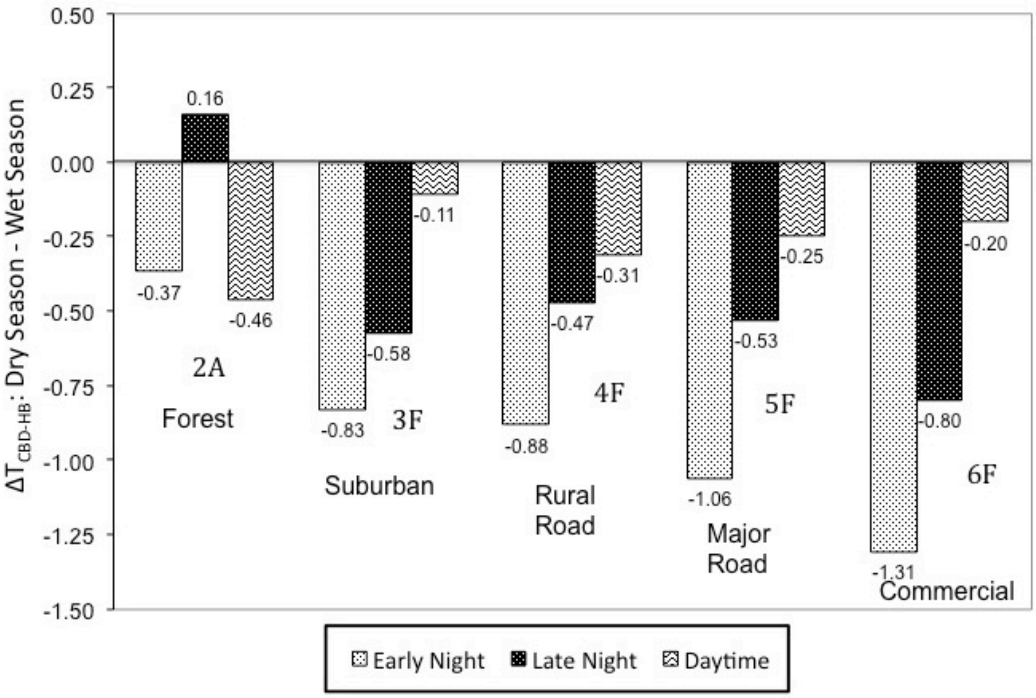

Figure 5. Difference between dry and wet season ΔT_{CBD-HB} data for HOBOs 2A, 3F, 4F, 5F, and 6F, stratified by time of day.

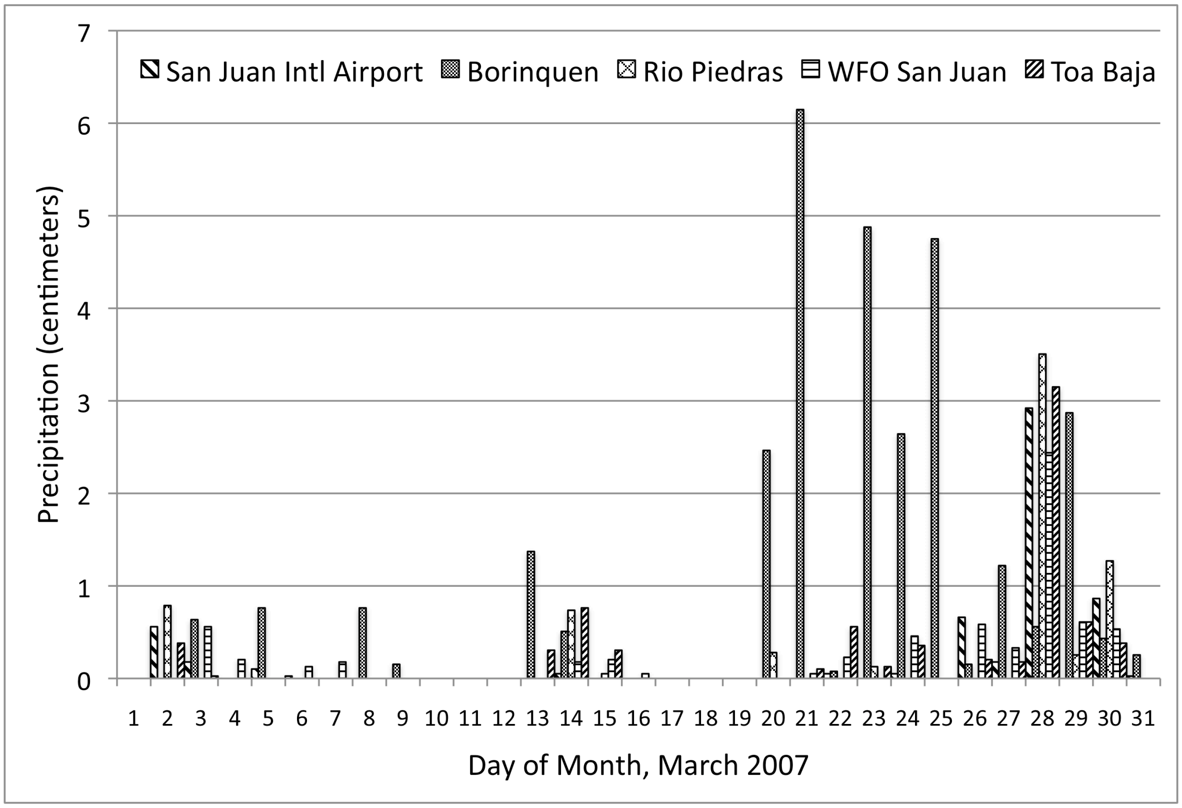

Figure 6. Daily precipitation totals for 3 stations within the San Juan Metropolitan Area during March of our data collection period.

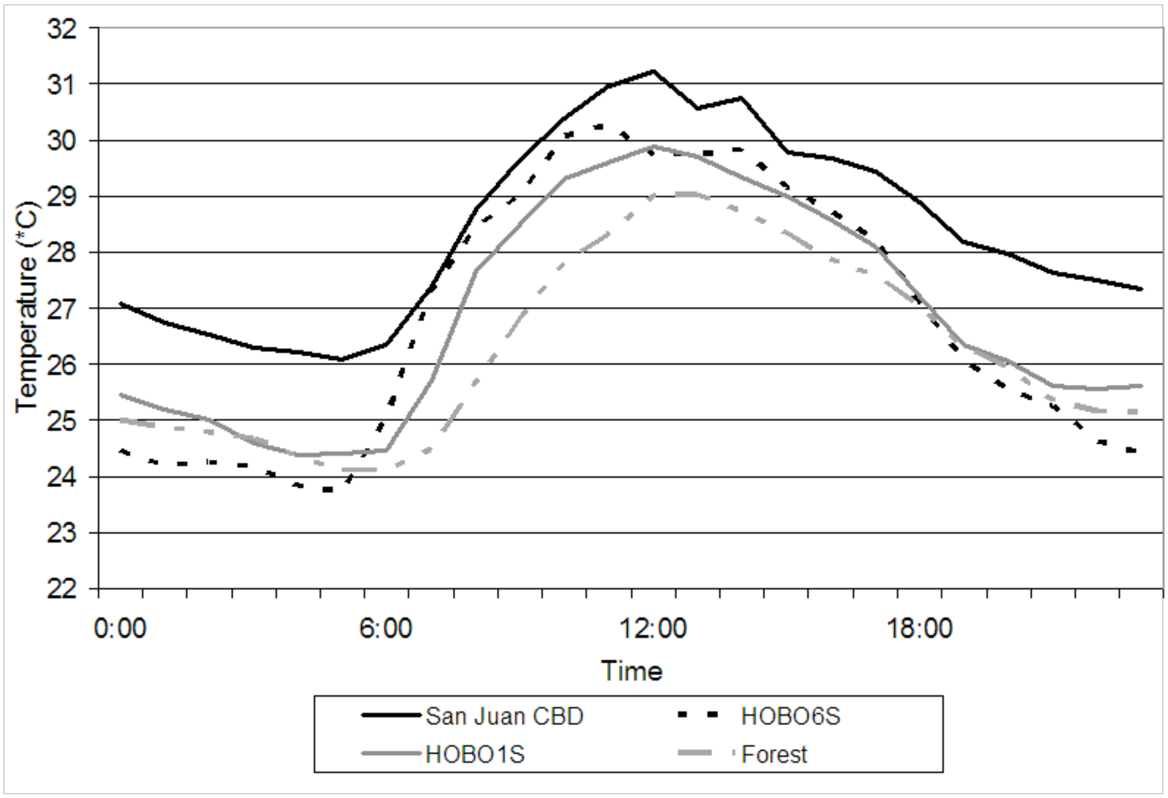

Figure 7. Diurnal temperature trends calculated as hourly averages from the summer data collection period for the central business district (CBD) of San Juan, forest location, HOBO 6S, and HOBO 1S. HOBO 1S is located west of a large abandoned agricultural field and HOBO 6S is located in a small mowed grassland site south of a large shopping center and northwest of the foothills of the Luquillo Mountains.

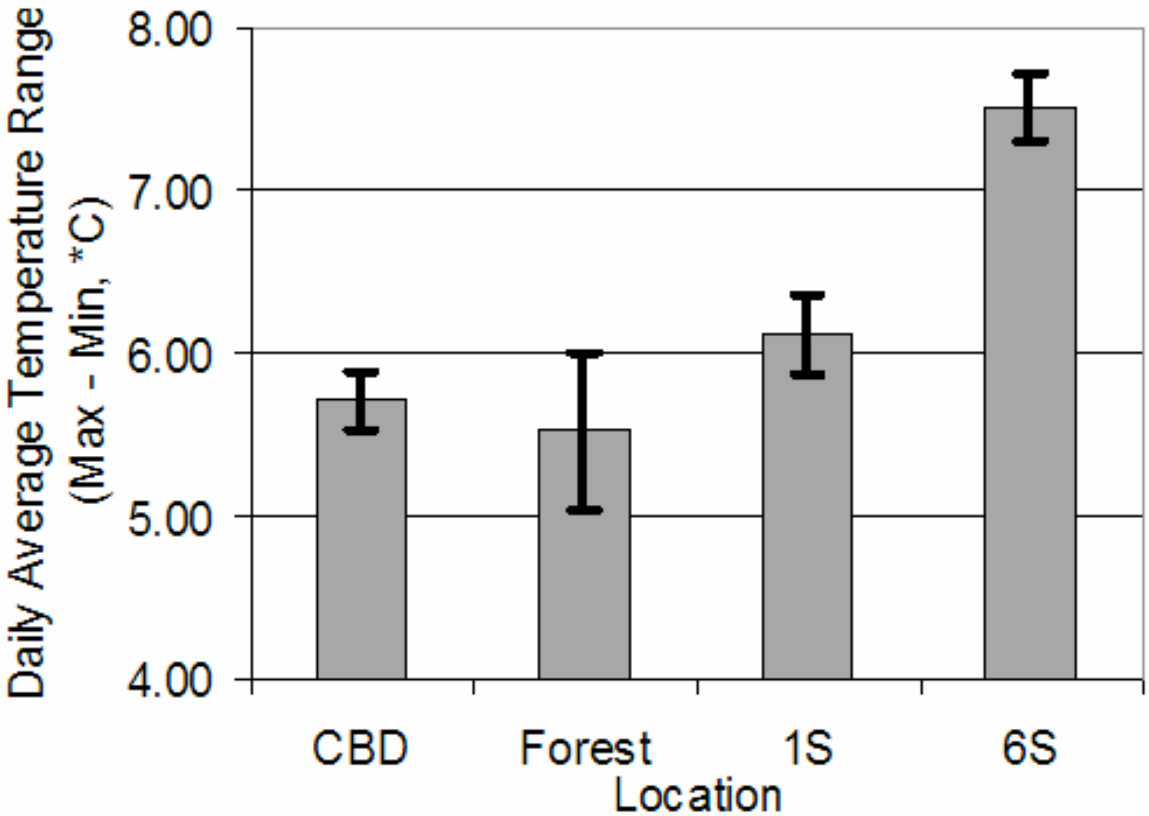

Figure 8. Diurnal temperature range, calculated as the average daily max – daily min, for data collected during the summer months at the central business district (CBD) of San Juan, the forest location, HOBO 1S, and HOBO 6S locations with standard error bars.

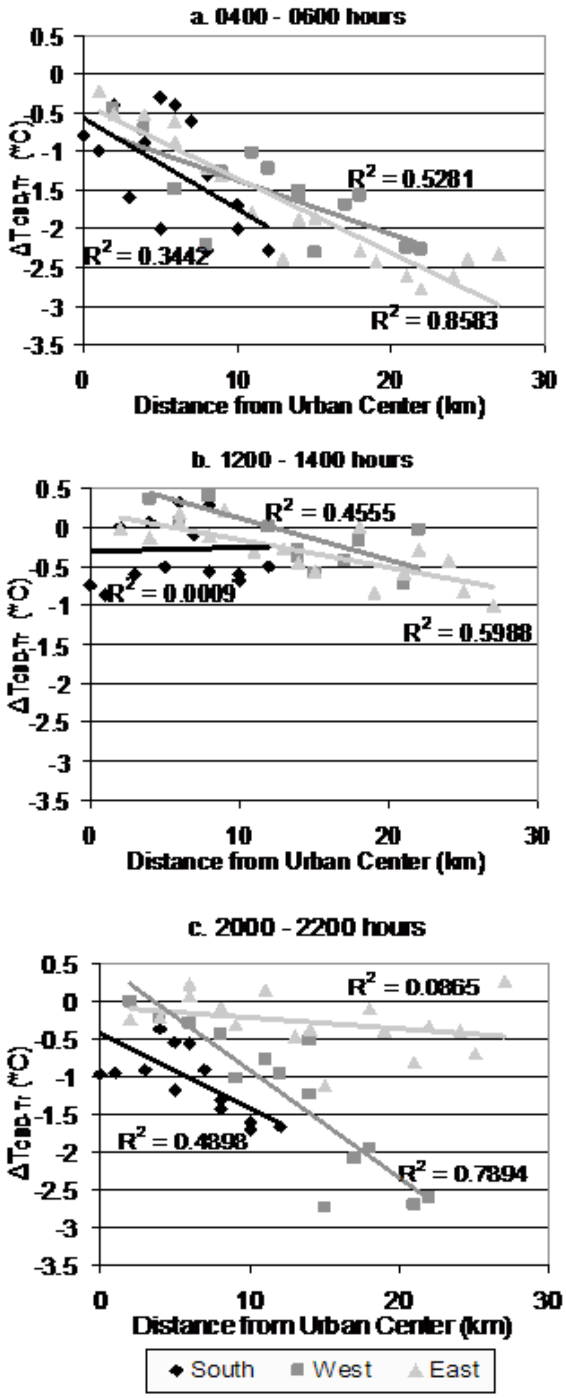

Figure 9a–c. $\Delta T_{CBD\text{-}Tr}$ trends along 3 routes emanating from the San Juan central business district to surrounding rural areas. Data from all three routes is stratified by time of day: (a.) 0400 – 0600. (b.) 1200 – 1400. (c.) 2000 – 2200.

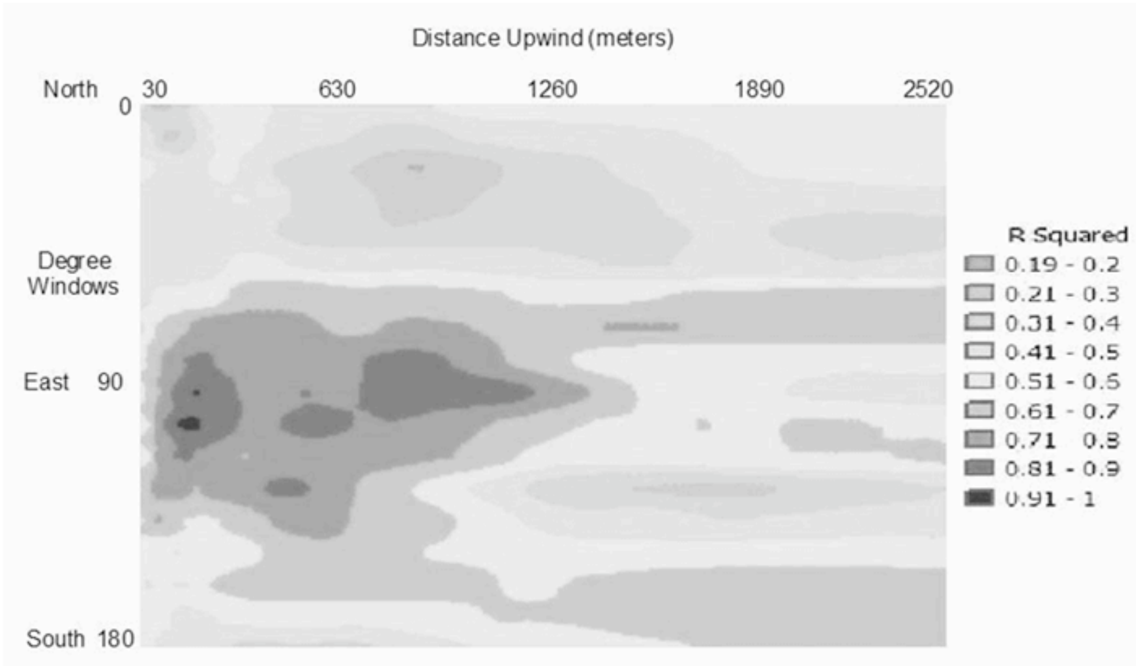

Figure 10. Isocorrelation plot showing correlation coefficients (R squared) for all 1512 regression analyses for ΔT_{CBD-HB} as a function of upwind vegetation. Degree windows 10-12 (91º - 120º), from 150 to 270 meters upwind, represent the 0.91 – 1.0 isocorrelation, and hence the best upwind fetch wedges for predicting temperature based on land-cover.

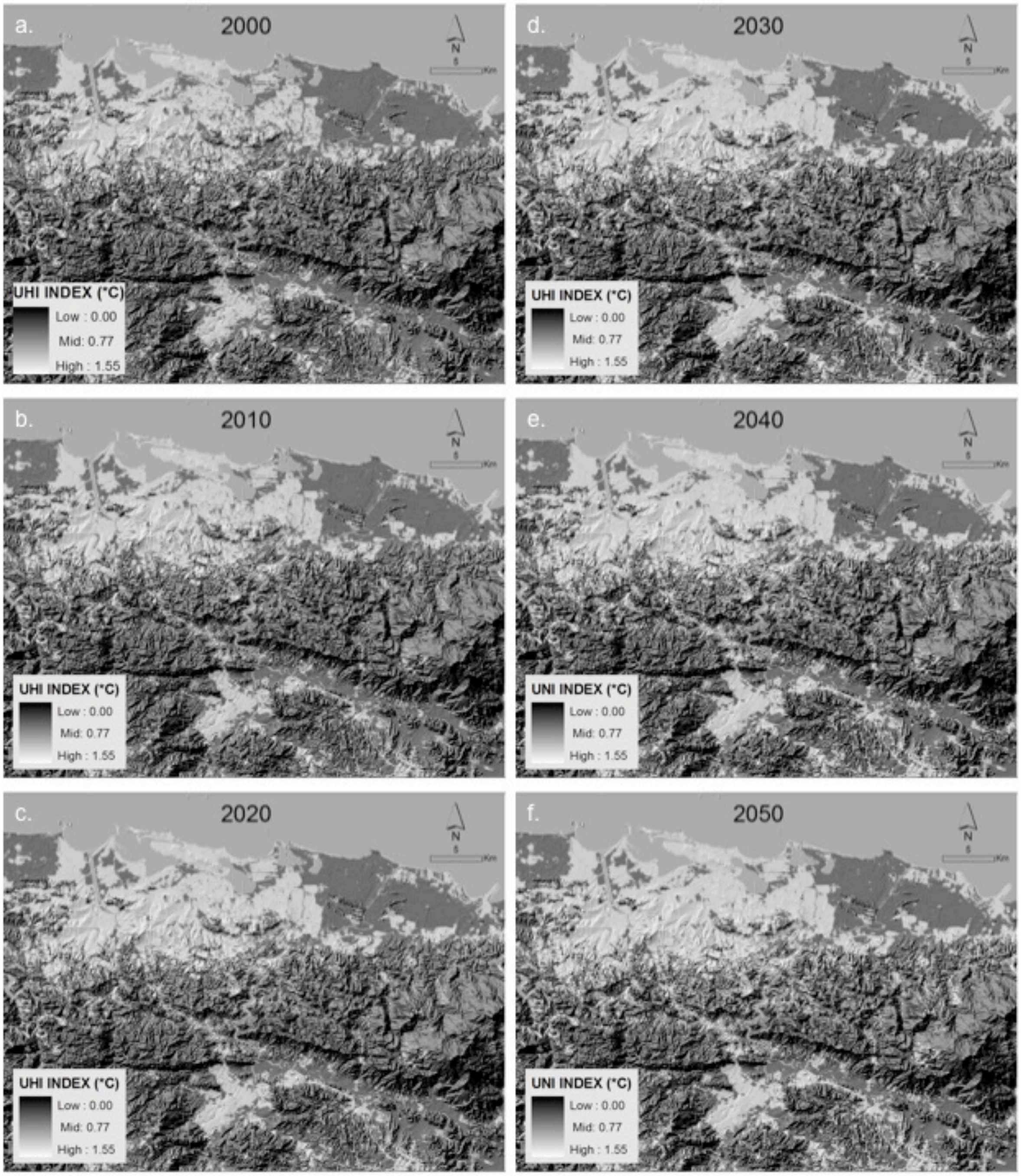

Figure 11a-f. Maps showing the current (a) and projected (b – f) UHI in northeastern Puerto Rico.